arXiv:1401.2447v3 [hep-ph] 26 Jun 2014

Higher-order electroweak corrections to the partial widths and branching ratios of the Z boson

Ayres Freitas

Pittsburgh Particle-physics Astro-physics & Cosmology Center (PITT-PACC), Department of Physics & Astronomy, University of Pittsburgh, Pittsburgh, PA 15260, USA

Abstract

Recently, the calculation of fermionic electroweak two-loop corrections to the total width of the Z boson and hadronic Z-peak cross-section in the Standard Model has been presented, where "fermionic" refers to diagrams with closed fermion loops. Here, these results are complemented by presenting contributions of the same order for the Z-boson partial widths, which are the last missing pieces for a complete description of Z-pole physics at the fermionic two-loop order. The definition of the relevant observables and the calculational techniques are described in detail. Numerical results are presented conveniently in terms of simple parametrization formulae. Finally, the remaining theoretical uncertainties from missing higher-order corrections are analyzed and found to be small compared to the current experimental errors.

1 Introduction

Electroweak precision observables (EWPOs) play a crucial role in testing the Standard Model (SM) at the quantum level and constraining physics beyond the SM. Some of the most important quantities in this context are the masses and widths of the W and Z bosons and the Z-boson couplings. The latter have been measured through the cross-section and polarization and angular asymmetries of the process $e^+e^- \to (Z) \to f\bar{f}$ at LEP1 and SLC, see *e. g.* Ref. [1]. Here f stands for any SM lepton or quark, except the top quark, and the symbol (Z) in brackets indicates s-channel exchange of an intermediate Z boson, which is unstable and thus not an asymptotic on-shell state. When computing theoretical predictions for the W and Z masses, widths and couplings, one has to take into account loop corrections, which depend on other elements of the SM, such as the top-quark mass, m_t, the Higgs boson mass, M_H, and the strong couplings constant, α_s. By combining direct measurements of these quantities with EWPOs in a global fit, one obtains a highly non-trivial and overconstrained test of the SM. On the other hand, a significant deviation between measurement and SM fit could be an indication for the presence of new particles in the loop corrections. For recent examples of such global fits and constraints on new physics, see *e. g.* Ref. [2–4].

Owing to the high precision of the experimental measurements, it is mandatory to include higher-order corrections beyond the one-loop approximation in the theory calculations. For the SM prediction of the W-boson mass, M_W, complete two-loop corrections, of order $\mathcal{O}(\alpha\alpha_\mathrm{s})$ and $\mathcal{O}(\alpha^2)$, are known [5–8]. In addition, partial three- and four-loop results, enhanced by powers of m_t, have been computed at order $\mathcal{O}(\alpha\alpha_\mathrm{s}^2)$ [9], $\mathcal{O}(\alpha^2\alpha_\mathrm{s}m_\mathrm{t}^4)$, $\mathcal{O}(\alpha^3 m_\mathrm{t}^6)$ [10], and $\mathcal{O}(\alpha\alpha_\mathrm{s}^3 m_\mathrm{t}^2)$ [11]. The same order of electroweak (EW) and QCD corrections are available for the leptonic effective weak mixing angle, $\sin^2\theta_\mathrm{eff}^\ell$ [12, 13], which describes the ratio of vector and axial-vector couplings of the Z boson to leptons. The effective weak mixing angles for quarks have been computed with *fermionic* two-loop corrections, which stem from diagrams with one or two closed fermion loops [13, 14], and the same partial three- and four-loop contributions mentioned above. The fermionic corrections are enhanced by powers of m_t and the large number of light fermion flavors, and thus expected to dominate over the *bosonic* corrections, which correspond to diagrams without closed fermion loop. This expectation is corroborated by experience from the calculation of M_W and $\sin^2\theta_\mathrm{eff}^\ell$, and thus the theory uncertainty from the missing bosonic $\mathcal{O}(\alpha^2)$ corrections is estimated to be relatively small [13, 14].

While the effective weak mixing angles are sensitive to the ratio of vector and axial-vector couplings of the Z boson to fermions, the overall strength of these couplings can be determined from the measurement of the partial widths, Γ_f, for the decay $Z \to f\bar{f}$. However, for the SM calculation of the Γ_f, even the fermionic two-loop corrections are not known, leading to potentially sizeable uncertainties in electroweak precision tests. The most precise existing result is based on a large-m_t expansion for the EW two-loop corrections, up to the next-to-leading order $\mathcal{O}(\alpha^2 m_\mathrm{t}^2)$ for final-state leptons and quarks of the first two generations [15], and only up to the leading $\mathcal{O}(\alpha^2 m_\mathrm{t}^4)$ term for the $Z \to b\bar{b}$ partial width [16]. As a first step to improve on this situation, Ref. [17] reported on the calculation of the fermionic two-loop contributions, without any approximation, to the branching ratio of the

Z-boson into $b\bar{b}$ and all hadronic final states, $R_b \equiv \Gamma_b/\Gamma_{\rm had}$.

This article describes the completion of the missing pieces to arrive at a complete description of Z-pole physics at the fermionic two-loop order. For this purpose, the full fermionic $\mathcal{O}(\alpha^2)$ corrections to the Z-boson partial widths have been calculated within the SM. Results for two related quantities, the total Z width, $\Gamma_{\rm Z}$, and the hadronic peak cross-section, $\sigma^0_{\rm had}$, have been presented recently in Ref. [18]. In this paper, details of the calculation are given, and numerical results for the partial widths, Γ_f, for all final states f are presented. It is demonstrated that the inclusion of these new results leads to predictions for Γ_f with a theory uncertainty safely below the experimental error.

The paper is organized as follows. In section 2, the definition of the relevant observables is discussed, with particular attention to gauge invariance and internal consistency to next-to-next-to-leading order in perturbation theory. Section 3 describes the methods used for the calculation of the EW two-loop diagrams, which use a combination of analytical and numerical techniques. Numerical results for the Z partial widths, as well as for various commonly used branching ratios, are shown in section 4. To make these results available to other researchers, simple parametrization formulae are provided, which accurately describe the full calculation within experimentally allowed ranges of the input parameters. Finally, section 5 is devoted to a discussion of the remaining theory error from unknown higher-order corrections.

2 Definition of the observables

Since the Z boson is unstable, it cannot be described as an asymptotic state, and the decay process $Z \to f\bar{f}$ is ill-defined in the usual formalism of perturbation theory. Instead, for the analysis of Z physics at LEP and SLC, one needs to consider the process $e^+e^- \to f\bar{f}$. Near the Z pole, the amplitude for $e^+e^- \to f\bar{f}$ can be written as a Laurent expansion about the complex pole $s_0 \equiv \overline{M}_{\rm Z}^2 - i\overline{M}_{\rm Z}\overline{\Gamma}_{\rm Z}$,

$$\mathcal{A}[e^+e^- \to f\bar{f}] = \frac{R}{s - s_0} + S + (s - s_0)S' + \ldots, \tag{1}$$

where $\overline{M}_{\rm Z}$ and $\overline{\Gamma}_{\rm Z}$ are the on-shell mass and width of the Z boson, respectively. It has been shown [19] that the coefficients $R, S, S', \ldots$ and the pole location s_0 are individually gauge-invariant, UV- and IR-finite, when soft and collinear real photon and gluon emission is included.

Note that, based on eq. (1), the s-dependence of the cross-section near the Z pole is given by $\sigma \propto [(s - \overline{M}_{\rm Z}^2)^2 + \overline{M}_{\rm Z}^2\overline{\Gamma}_{\rm Z}^2]^{-1}$, whereas in experimental analyses a Breit-Wigner function with a running (energy-dependent) width is being employed, $\sigma \propto [(s - M_{\rm Z}^2)^2 + s^2\Gamma_{\rm Z}^2/M_{\rm Z}^2]^{-1}$. Due to these different parametrizations, the experimental mass and width, $M_{\rm Z}$ and $\Gamma_{\rm Z}$, differ from the pole mass and width, $\overline{M}_{\rm Z}$ and $\overline{\Gamma}_{\rm Z}$, by a fixed factor:

$$\overline{M}_{\rm Z} = M_{\rm Z}/\sqrt{1 + \Gamma_{\rm Z}^2/M_{\rm Z}^2}\,, \qquad \overline{\Gamma}_{\rm Z} = \Gamma_{\rm Z}/\sqrt{1 + \Gamma_{\rm Z}^2/M_{\rm Z}^2}\,. \tag{2}$$

Numerically, this leads to $\overline{M}_{\rm Z} \approx M_{\rm Z} - 34$ MeV and $\overline{\Gamma}_{\rm Z} \approx \Gamma_{\rm Z} - 0.9$ MeV.

The total width, $\overline{\Gamma}_{\rm Z}$, is related to the imaginary part of the complex pole s_0. It can be obtained by requiring that the Z propagator has a pole for $s = s_0$, *i. e.*

$$s_0 - \overline{M}_{\rm Z}^2 + \Sigma_{\rm Z}(s_0) = 0, \tag{3}$$

where $\Sigma_{\rm Z}(s)$ is the transverse part of the Z self-energy. The real and imaginary part of this equation, respectively, lead to

$$\mathrm{Re}\,\Sigma_{\rm Z}(s_0) = 0, \qquad\qquad \overline{\Gamma}_{\rm Z} = \frac{1}{\overline{M}_{\rm Z}} \mathrm{Im}\,\Sigma_{\rm Z}(s_0). \tag{4a,b}$$

Expanding eq. (4b) up to next-to-next-to-leading order in α, with the power counting $\overline{\Gamma}_{\rm Z} \sim \mathcal{O}(\alpha)$, and using eq. (4a), one obtains

$$\begin{aligned}\overline{\Gamma}_{\rm Z} = \frac{1}{\overline{M}_{\rm Z}} \Big\{ & \mathrm{Im}\,\Sigma_{\rm Z(1)} \;+\; \mathrm{Im}\,\Sigma_{\rm Z(2)} - (\mathrm{Im}\,\Sigma_{\rm Z(1)})(\mathrm{Re}\,\Sigma'_{\rm Z(1)}) \\ & + \mathrm{Im}\,\Sigma_{\rm Z(3)} + (\mathrm{Im}\,\Sigma_{\rm Z(1)})\big[(\mathrm{Re}\,\Sigma'_{\rm Z(1)})^2 - \mathrm{Re}\,\Sigma'_{\rm Z(2)}\big] - (\mathrm{Im}\,\Sigma_{\rm Z(2)})(\mathrm{Re}\,\Sigma'_{\rm Z(1)}) \\ & - \tfrac{1}{2}\overline{M}_{\rm Z}\overline{\Gamma}_{\rm Z}(\mathrm{Im}\,\Sigma_{\rm Z(1)})(\mathrm{Im}\,\Sigma''_{\rm Z(1)}) \Big\}_{s=\overline{M}_{\rm Z}^2} .\end{aligned} \tag{5}$$

Here the subscripts in brackets indicate the loop order and $\Sigma'_{\rm Z}$ is the derivative of $\Sigma_{\rm Z}$. Making use of optical theorem, one can relate the imaginary part of the self-energy to the decay process $Z \to f\bar{f}$, which gives

$$\mathrm{Im}\,\Sigma_{\rm Z} = \frac{1}{3\overline{M}_{\rm Z}} \sum_f \sum_{\rm spins} \int d\Phi \, \left(|v_f|^2 + |a_f|^2\right), \tag{6}$$

where v_f and a_f are the effective vector and axial-vector couplings, respectively, of the $Zf\bar{f}$ vertex, which include EW vertex corrections and Z–γ mixing contributions. Final-state QED and QCD corrections can be added via factorized radiator functions $\mathcal{R}_{\rm V,A}$, so that one arrives at

$$\overline{\Gamma}_{\rm Z} = \sum_f \overline{\Gamma}_f \,, \qquad \overline{\Gamma}_f = \frac{N_c^f \overline{M}_{\rm Z}}{12\pi} \Big[\mathcal{R}_{\rm V}^f F_{\rm V}^f + \mathcal{R}_{\rm A}^f F_{\rm A}^f \Big]_{s=\overline{M}_{\rm Z}^2} \,, \tag{7}$$

$$\begin{aligned} F_{\rm V}^f = {} & v_{f(0)}^2 \big[1 - \mathrm{Re}\,\Sigma'_{\rm Z(1)} - \mathrm{Re}\,\Sigma'_{\rm Z(2)} + (\mathrm{Re}\,\Sigma'_{\rm Z(1)})^2\big] + 2\,\mathrm{Re}\,(v_{f(0)} v_{f(1)}) \big[1 - \mathrm{Re}\,\Sigma'_{\rm Z(1)}\big] \\ & + 2\,\mathrm{Re}\,(v_{f(0)} v_{f(2)}) + |v_{f(1)}|^2 - \tfrac{1}{2}\overline{M}_{\rm Z}\overline{\Gamma}_{\rm Z} v_{f(0)}^2 \,\mathrm{Im}\,\Sigma''_{\rm Z(1)} \,, \end{aligned} \tag{8}$$

$$\begin{aligned} F_{\rm A}^f = {} & a_{f(0)}^2 \big[1 - \mathrm{Re}\,\Sigma'_{\rm Z(1)} - \mathrm{Re}\,\Sigma'_{\rm Z(2)} + (\mathrm{Re}\,\Sigma'_{\rm Z(1)})^2\big] + 2\,\mathrm{Re}\,(a_{f(0)} a_{f(1)}) \big[1 - \mathrm{Re}\,\Sigma'_{\rm Z(1)}\big] \\ & + 2\,\mathrm{Re}\,(a_{f(0)} a_{f(2)}) + |a_{f(1)}|^2 - \tfrac{1}{2}\overline{M}_{\rm Z}\overline{\Gamma}_{\rm Z} a_{f(0)}^2 \,\mathrm{Im}\,\Sigma''_{\rm Z(1)} \,, \end{aligned} \tag{9}$$

where $N_c^f = 3(1)$ for quarks (leptons). The functions $\mathcal{R}_{\rm V,A}$ have been computed including higher-order QCD corrections up to $\mathcal{O}(\alpha_{\rm s}^4)$ in the limit of massless quarks and $\mathcal{O}(\alpha_{\rm s}^3)$ for the kinematic mass corrections [20, 21]. Furthermore, $\mathcal{O}(\alpha^2)$ QED corrections have been obtained in Ref. [22]. The complete expressions used in this work are given in the appendix.

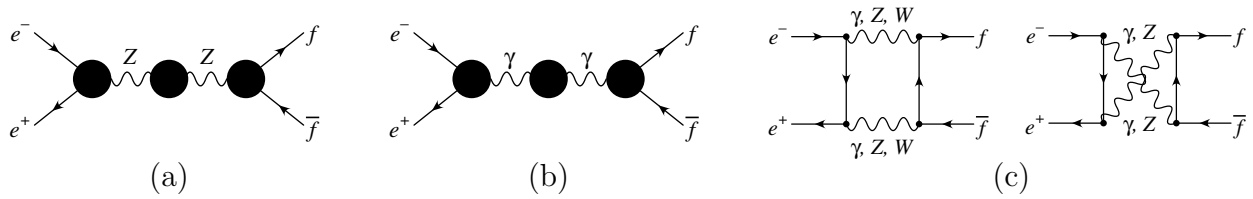

Figure 1: *Generic diagrams for s-channel Z-boson (a) and photon (b) exchange, as well as box graphs (c). The blobs indicate self-energy and vertex loop corrections.*

However, the factorization between final-state QCD/QED corrections and EW loop corrections from massive gauge-boson exchange is not exact, but there are additional non-factorizable contributions from irreducible vertex diagrams. The leading non-factorizable corrections at $\mathcal{O}(\alpha\alpha_s)$ have been computed in Ref. [23, 24], and were found to be relatively small, but not negligible compared to the current experimental uncertainty.

The hadronic peak cross section, $\sigma^0_{\rm had}$, is phenomenologically defined as the total cross section for $e^+e^- \to (Z) \to$ hadrons for $s = M_{\rm Z}^2$, after subtraction of s-channel photon exchange and box diagram contributions, see Fig. 1 (b,c), and de-convolution of initial-state QED radiation [1,25]. The notation (Z) in brackets is supposed to indicate that the unstable Z-boson is not an asymptotic state. As mentioned above, the experimental collaborations commonly parametrize the cross section, $\sigma_{\rm had} = \sigma[e^+e^- \to (Z) \to \text{hadrons}]$ near the Z peak through a Breit-Wigner form with an energy-dependent width,

$$\sigma_{\rm had}(s) = \sigma^0_{\rm had} \frac{s\Gamma_{\rm Z}^2}{(s - M_{\rm Z}^2)^2 + s^2\Gamma_{\rm Z}^2/M_{\rm Z}^2}, \tag{10}$$

so that $\sigma^0_{\rm had} = \sigma_{\rm had}(M_{\rm Z}^2)$. Note that one obtains the same result at the location of the complex pole mass: $\sigma^0_{\rm had} = \sigma_{\rm had}(\overline{M}_{\rm Z}^2)$.

On the theory side, the hadronic peak cross section is computed from the amplitude in eq. (1). The latter can be written as $\mathcal{A}(s) = \mathcal{A}_{\rm Z}(s) + \mathcal{A}_\gamma(s) + B(s)$, where $\mathcal{A}_{\rm Z}$ and $\mathcal{A}_\gamma$ are the terms from Z-boson and photon exchange, respectively, and B denotes EW box diagram contributions. Then

$$\sigma_{\rm had} = \frac{1}{64\pi^2 s} \sum_{f=u,d,c,s,b} \int d\Omega \, \big|\mathcal{A}_{\rm Z}(s)\big|^2. \tag{11}$$

Expanding $\mathcal{A}_{\rm Z}$ about the complex pole s_0 as in eq. (1), the gauge-invariant coefficients read, including electroweak next-to-next-to-leading order corrections (final-state radiation will be added later),

$$\begin{aligned} R_{\rm Z} = \; & z^\mu_{e(0)} z^\mu_{f(0)} \big[1 - \Sigma'_{\rm Z(1)} - \Sigma'_{\rm Z(2)} + (\Sigma'_{\rm Z(1)})^2 + i\overline{M}_{\rm Z}\overline{\Gamma}_{\rm Z}\Sigma''_{\rm Z(1)}\big] \\ & + \big[z^\mu_{e(1)} z^\mu_{f(0)} + z^\mu_{e(0)} z^\mu_{f(1)}\big]\big[1 - \Sigma'_{\rm Z(1)}\big] + z^\mu_{e(2)} z^\mu_{f(0)} + z^\mu_{e(0)} z^\mu_{f(2)} + z^\mu_{e(1)} z^\mu_{f(1)} \\ & - i\overline{M}_{\rm Z}\overline{\Gamma}_{\rm Z}\big[z^{\mu\prime}_{e(1)} z^\mu_{f(0)} + z^\mu_{e(0)} z^{\mu\prime}_{f(1)}\big], \end{aligned} \tag{12}$$

$$S_{\rm Z} = z^{\mu\,\prime}_{e(1)} z^{\mu}_{f(0)} + z^{\mu}_{e(0)} z^{\mu\,\prime}_{f(1)} + \tfrac{1}{2} z^{\mu}_{e(0)} z^{\mu}_{f(0)} \Sigma''_{{\rm Z}(1)}, \tag{13}$$

$$S'_{\rm Z} = 0. \tag{14}$$

Here the consistent power counting $\overline{\Gamma}_{\rm Z} = \mathcal{O}(\alpha)$ has been used, so that $R_{\rm Z}$ is needed to two-loop order, while it is sufficient to compute S and S' to one-loop and tree-level order, respectively. $z^{\mu}_{f(n)}$ denotes the n-loop correction to the effective $Zf\bar{f}$ vertex, *i. e.*

$$z^{\mu}_{f(n)} = v_{f(n)} \gamma^{\mu} + a_{f(n)} \gamma^{\mu} \gamma^{5}. \tag{15}$$

Inserting the expressions in eqs. (12)–(14) into eq. (10) and setting $s = \overline{M}^2_{\rm Z}$, one finds

$$\sigma^0_{\rm had} = \sum_{f=u,d,c,s,b} \frac{N^f_c}{12\pi \overline{\Gamma}^2_{\rm Z}} \Big[\big(F^e_{\rm V} + F^e_{\rm A}\big)\big(F^f_{\rm V} + F^f_{\rm A}\big) + \big(v^2_{e(0)} + a^2_{e(0)}\big)\big(v^2_{f(0)} + a^2_{f(0)}\big) \delta X_{(2)} \Big]_{s=\overline{M}^2_{\rm Z}}, \tag{16}$$

where

$$\delta X_{(2)} = -(\mathrm{Im}\, \Sigma'_{{\rm Z}(1)})^2 - 2 \overline{\Gamma}_{\rm Z} \overline{M}_{\rm Z}\, \mathrm{Im}\, \Sigma''_{{\rm Z}(1)}\,. \tag{17}$$

So far, this expression for $\sigma^0_{\rm had}$ only accounts for the virtual EW corrections. As for the total width, final-state QED and QCD radiation can be included through the radiator functions $\mathcal{R}_{\rm V,A}$. The final result for $\sigma^0_{\rm had}$ can then be written as

$$\sigma^0_{\rm had} = \sum_{f=u,d,c,s,b} \frac{12\pi}{\overline{M}^2_{\rm Z}} \frac{\overline{\Gamma}_e \overline{\Gamma}_f}{\overline{\Gamma}^2_{\rm Z}} (1 + \delta X)\,. \tag{18}$$

The correction factor δX occurs first at two-loop level, see eq. (17), and can be traced to the last two terms in the first line of eq. (12). Its existence has been realized earlier in Ref. [26], although eq. (17) differs from the expression given there. This difference stems from the non-resonant term eq. (13), which has not been included in Ref. [26].

Note that v_f, a_f and Σ_Z as defined above include γ–Z mixing contributions, see Fig. 2. Specifically,

$$v_f(s) = v^{\rm Z}_f(s) - v^{\gamma}_f(s)\, \frac{\Sigma_{\gamma Z}(s)}{s + \Sigma_{\gamma\gamma}(s)}, \tag{19}$$

$$a_f(s) = a^{\rm Z}_f(s) - a^{\gamma}_f(s)\, \frac{\Sigma_{\gamma Z}(s)}{s + \Sigma_{\gamma\gamma}(s)}, \tag{20}$$

$$\Sigma_Z(s) = \Sigma_{ZZ}(s) - \frac{[\Sigma_{\gamma Z}(s)]^2}{s + \Sigma_{\gamma\gamma}(s)}, \tag{21}$$

where $v^{\rm Z}_f$ and $a^{\rm Z}_f$ are the one-particle irreducible $Zf\bar{f}$ vector and axial-vector vertex contributions, respectively, and v^{γ}_f and a^{γ}_f are their equivalent for the $\gamma f\bar{f}$ vertex. The symbols $\Sigma_{V_1V_2}$ denote the one-particle irreducible corrections to the V_1–V_2 self-energy.

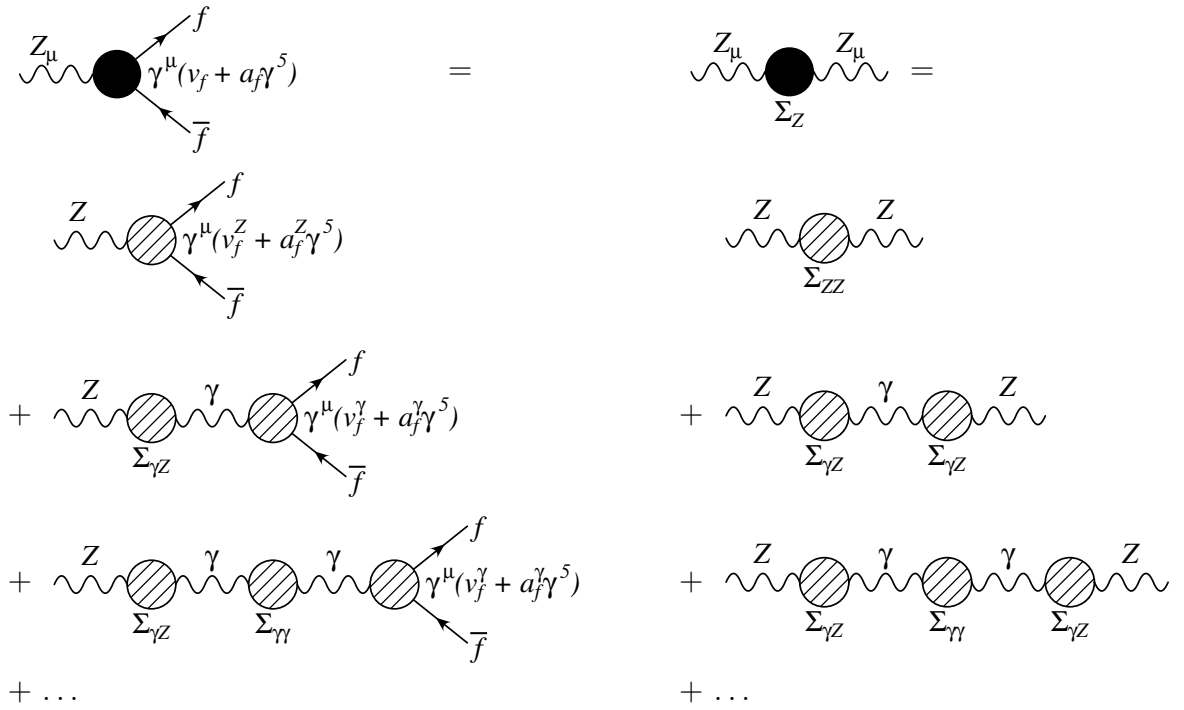

Figure 2: *Decomposition of the effective $Zf\bar{f}$ vertex and Z self-energy into one-particle irreducible building blocks, indicated by the hatched blobs.*

3 Calculation of fermionic two-loop corrections

In the calculation of the electroweak two-loop corrections with one or two closed fermion loops, the masses and Yukawa couplings of all fermions except the top quark have been neglected. [For the one-loop and $\mathcal{O}(\alpha\alpha_s)$ corrections, the finite bottom-quark mass has been retained.] Moreover, the quark mixing matrix is assumed to be diagonal. The diagrams for the $Zf\bar{f}$ vertex corrections and for the renormalization terms have been generated with FeynArts 3.3 [27]. Dimensional regularization is used for defining potentially UV-divergent loop integrals. The vector and axial-vector form factors, $v_{f(n)}$ and $a_{f(n)}$, have been singled out by contraction with suitable projection operators,

$$v_f(k^2) = \frac{1}{2(2-d)k^2}\,\mathrm{Tr}[\gamma_\mu \not{p}_1\, z_f^\mu(k^2)\, \not{p}_2], \tag{22}$$

$$a_f(k^2) = \frac{1}{2(2-d)k^2}\,\mathrm{Tr}[\gamma_5\, \gamma_\mu \not{p}_1\, z_f^\mu(k^2)\, \not{p}_2], \tag{23}$$

where d is the space-time dimension and $p_{1,2}$ are the momenta of the external fermions. The resulting expression contain only scalar loop integrals, which however may still contain non-trivial structures of scalar products in their numerators.

For the purpose of the work presented here, the on-shell renormalization scheme is employed. In this scheme, the renormalized squared masses are defined at the real part of the propagator poles, see also eq. (1). Specifically, for the $\mathcal{O}(\alpha^2)$ corrections, mass counterterms

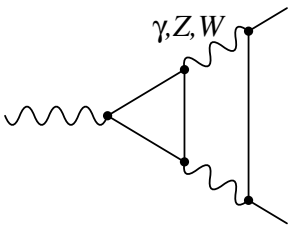

Figure 3: *Generic two-loop vertex diagram with triangle fermion sub-loop.*

are needed for $\overline{M}_{\rm W}$, $\overline{M}_{\rm Z}$, and $m_{\rm t}$. The electromagnetic charge is defined as the coupling strength of the $\gamma f \bar{f}$ in the limit of zero photon momentum, and the *on-shell* weak mixing angle is defined through the ratio of the renormalized W and Z masses, $s_{\rm w} = 1 - \overline{M}_{\rm W}^2/\overline{M}_{\rm Z}^2$. Finally, wave function renormalization constants for the external fermions are needed. Detailed expressions for the relevant counterterms are given in Ref. [7]. When computing the Z decay width, one cannot define a physical wave-function or field-strength renormalization of the incoming Z boson, since it is unstable and thus not an asymptotic state*. Instead, UV-divergencies associated in the incoming Z-boson line are canceled by the terms involving the derivative of the self-energy, $\Sigma'_{\rm Z}$, in eqs. (8), (9).

Two-loop self-energy integrals and vertex integrals with sub-loop self-energy bubbles have been evaluated with the method illustrated in section 3.2 of Ref. [13]. In this approach, the loop integrals are reduced to a small set of master integrals using a generalization of Passarino-Veltman reduction [29], as well as integration-by-parts [30] and Lorentz identities [31]. The master integrals are then evaluated using very efficient one-dimensional numerical integrations [13, 32].

For the computation of $\Sigma'_{\rm Z}$, derivatives of self-energy integrals are needed. To illustrate their evaluation, let us write a two-loop self-energy master integral in the form

$$T(p^2; m_1^2, m_2^2, m_3^2, m_4^2, m_5^2; \nu_1, \nu_2, \nu_3, \nu_4, \nu_5) = -\frac{(4\pi^2\mu^2)^{4-d}}{\pi^4} \times \int \frac{d^d q_1 d^d q_2}{[q_1^2 - m_1^2]^{\nu_1}[(q_1+p)^2 - m_2^2]^{\nu_2}[(q_1-q_2)^2 - m_3^2]^{\nu_3}[q_2^2 - m_4^2]^{\nu_4}[(q_2+p)^2 - m_5^2]^{\nu_5}} \quad (24)$$

where p is the external momentum. The derivative with respect to p^2 can be expressed in terms of the same functions:

$$\frac{\partial T}{\partial(p^2)} = \frac{1}{2p^2} p^\mu \frac{\partial T}{\partial p^\mu} = -\frac{1}{2p^2}\big[(\nu_2+\nu_5)T - \nu_2 T(\nu_1 - 1, \nu_2 + 1) - \nu_5 T(\nu_4 - 1, \nu_5 + 1) + (m_2^2 - m_1^2 + p^2)T(\nu_2 + 1) + (m_5^2 - m_4^2 + p^2)T(\nu_5 + 1)\big]. \quad (25)$$

With the help of integration-by-parts identities, the resulting integrals can again be reduced to a basic set with all ν_i either 1 or 0.

*For a technical definition of the of the field-strength renormalization of unstable particles, see *e. g.* Ref. [28].

For vertex diagrams with sub-loop triangles, see Fig. 3, the numerical integration technique of Ref. [33] has been used. This method is based on a direct integration in Feynman parameter space, without prior tensor reduction, and using a deformation of integration contours into the complex plane to avoid poles from physical thresholds. Where applicable, results for individual diagrams obtained with this approach have been compared to Ref. [14].

In this context, it should be pointed out that diagrams with fermion triangle sub-loop involve chiral couplings that lead to Dirac traces of the form

$$\mathrm{tr}\{\gamma^\alpha\gamma^\beta\gamma^\gamma\gamma^\delta\gamma_5\} = 4i\epsilon^{\alpha\beta\gamma\delta}. \tag{26}$$

Within dimensional regularization, eq. (26) is inconsistent with the anticommutation rule $\{\gamma^\mu, \gamma_5\} = 0$. However, it can be shown (see for instance Ref. [34]) that contributions proportional to epsilon tensors of the form (26) are separately gauge-invariant and UV-finite, and thus they can be computed in four dimensions with a well-defined result. In order to avoid difficulties due to spurious IR-singularities from diagrams with massless photons, a small photon mass is introduced [13]. The sum of all triangle sub-loop diagrams is IR-finite, so that any remaining contribution from the small photon mass is power suppressed.

Additional checks have been performed for the complete result, combining all building blocks, including two-loop vertex diagrams, counterterms for the renormalization and reducible terms (*i. e.* $\mathcal{O}(\alpha^2)$ contributions that factorize into a product of one-loop factors). The UV- and IR-finiteness has been checked analytically within dimensional regularization. The final expressions for the vector and axial-vector form factors, $v_{f(2)}$ and $a_{f(2)}$, can also be used to evaluate the effective weak mixing angle $\sin^2\theta^f_{\mathrm{eff}} = \frac{1}{4}(1 + \mathrm{Re}\{v_l/a_l\})$, and very good agreement with the literature has been obtained for $f = \ell$ [12] and $f = b$ [14]. Furthermore, the fermionic two-loop result for R_b from Ref. [17] has been reproduced with good accuracy. In all of these comparisons, the agreement is better than the intrinsic uncertainty from numerical integration errors.

4 Numerical results

In this section, numerical results for the partial widths $\Gamma_f \equiv \Gamma(Z \to f\bar{f})$, their ratios, the total Z width Γ_{Z}, and the hadronic peak cross-section σ_{had} are presented. Although the calculation is performed using the complex-pole definition of the gauge-boson masses, see section 2, the numerical results are given in terms of the running width scheme, *i. e.* M_{Z} and Γ_{Z} in eq. (2).

All currently known perturbative corrections are included in the result:

- $\mathcal{O}(\alpha)$ and and fermionic $\mathcal{O}(\alpha^2)$ EW contributions (from this work);
- $\mathcal{O}(\alpha\alpha_{\mathrm{s}})$ corrections to internal gauge-boson self-energies [5] (which have been re-computed for this work);
- leading three- and four-loop corrections in the large-m_{t} limit, of order $\mathcal{O}(\alpha_{\mathrm{t}}\alpha_{\mathrm{s}}^2)$ [9], $\mathcal{O}(\alpha_{\mathrm{t}}^2\alpha_{\mathrm{s}})$, $\mathcal{O}(\alpha_{\mathrm{t}}^3)$ [10], and $\mathcal{O}(\alpha_{\mathrm{t}}\alpha_{\mathrm{s}}^3)$ [11], where $\alpha_{\mathrm{t}} \equiv \alpha m_{\mathrm{t}}^2$;

Parameter	Value	Parameter	Value
$M_{\rm Z}$	91.1876 GeV	$m_{\rm b}^{\overline{\rm MS}}$	4.20 GeV
$\Gamma_{\rm Z}$	2.4952 GeV	$m_{\rm c}^{\overline{\rm MS}}$	1.275 GeV
$M_{\rm W}$	80.385 GeV	m_τ	1.777 GeV
$\Gamma_{\rm W}$	2.085 GeV	$\Delta\alpha$	0.05900
$M_{\rm H}$	125.7 GeV	$\alpha_{\rm s}(M_{\rm Z})$	0.1184
$m_{\rm t}$	173.2 GeV	G_μ	1.16638×10^{-5} GeV^{-2}

Table 1: *Input parameters used in the numerical analysis, from Refs. [2, 4, 35, 36].*

- final-state QED and QCD (for quark final states) radiation up to $\mathcal{O}(\alpha^2)$, $\mathcal{O}(\alpha\alpha_{\rm s})$ and $\mathcal{O}(\alpha_{\rm s}^4)$ [20–22], which are incorporated through the radiator functions $\mathcal{R}_{\rm V,A}$;
- non-factorizable $\mathcal{O}(\alpha\alpha_{\rm s})$ vertex contributions [23, 24], which account for the fact that the factorization between EW corrections in $F_{\rm V,A}$ and final-state radiation effects in $\mathcal{R}_{\rm V,A}$ is not exact.

Light fermion masses m_f, $f \neq t$, have been neglected everywhere except for a non-zero b quark mass in the $\mathcal{O}(\alpha)$ and $\mathcal{O}(\alpha\alpha_{\rm s})$ contributions, non-zero bottom, charm and tau masses in the radiators $\mathcal{R}_{\rm V,A}$. The top-quark mass, $m_{\rm t}$, has been defined in the on-shell scheme, while the $\overline{\rm MS}$-scheme has been used for $m_{\rm c}$ and $m_{\rm b}$.

Owing to the renormalization scheme used here, the EW corrections are obtained in terms of the electromagnetic coupling α, rather than the Fermi constant G_μ, as expansion parameter. However, in a second step, the measured value of G_μ is used to compute $M_{\rm W}$ within the SM, leading to a prediction of the (partial) Z width and cross-section in terms of $M_{\rm Z}$, $M_{\rm H}$, $m_{\rm t}$, $m_{\rm b}^{\overline{\rm MS}}$, $m_{\rm c}^{\overline{\rm MS}}$, m_τ, G_μ, α, $\alpha_{\rm s}$ and $\Delta\alpha$. Here $\Delta\alpha$ describes the shift in the electromagnetic coupling between the scales $q^2 = 0$ and $M_{\rm Z}^2$ due to light fermion loops, $\alpha(M_{\rm Z}^2) = \alpha(0)/(1 - \Delta\alpha)$. While the contribution to $\Delta\alpha$ from leptons has been computed perturbatively up to three-loop level [35], $\Delta\alpha_{\rm lept}(M_{\rm Z}) = 0.0314976$, the quark loops at low scales lead to non-perturbative contributions that have to be taken from experimental data, see *e. g.* [36], and the value $\Delta\alpha_{\rm had}^{(5)}(M_{\rm Z}) = 0.02750$ is adopted here. The numerical input values used in this section are listed in Tab. 1.

Results for the total width, $\Gamma_{\rm Z}$, and hadronic peak cross-section, $\sigma_{\rm had}^0$, have been presented in Ref. [18]. In the following subsections, numerical results for the partial widths and branching ratios will be discussed.

4.1 Partial widths

Results for the contribution of the different loop orders to various partial widths are shown in Tab. 2 for a fixed value of $M_{\rm W}$ (*i. e.* G_μ is not used as an input parameter here). As evident from the table, the two-loop EW corrections are sizeable, of the same order as the $\mathcal{O}(\alpha\alpha_{\rm s})$ terms.

Γ_i [MeV]	Γ_e	Γ_ν	Γ_d	Γ_u	Γ_b	Γ_Z
$\mathcal{O}(\alpha)$	2.274	6.176	9.724	5.804	3.863	60.26
$\mathcal{O}(\alpha\alpha_\mathrm{s})$	0.288	0.458	1.276	1.156	2.006	9.11
$\mathcal{O}(\alpha_\mathrm{t}\alpha_\mathrm{s}^2,\ \alpha_\mathrm{t}\alpha_\mathrm{s}^3,\ \alpha_\mathrm{t}^2\alpha_\mathrm{s},\ \alpha_\mathrm{t}^3)$	0.038	0.059	0.191	0.170	0.190	1.20
$\mathcal{O}(N_f^2\alpha^2)$	0.244	0.416	0.698	0.528	0.694	5.13
$\mathcal{O}(N_f\alpha^2)$	0.121	0.186	0.494	0.494	0.144	3.04

Table 2: *Loop contributions, in units of MeV, to the partial and total Z widths with fixed M_W as input parameter. Here N_f and N_f^2 refer to corrections with one and two closed fermion loops, respectively, and $\alpha_\mathrm{t} = \alpha m_\mathrm{t}^2$. In all rows the radiator functions $\mathcal{R}_\mathrm{V,A}$ with known contributions through $\mathcal{O}(\alpha_\mathrm{s}^4)$, $\mathcal{O}(\alpha^2)$ and $\mathcal{O}(\alpha\alpha_\mathrm{s})$ are included.*

If one uses G_μ as an input to compute M_W, using the results from Ref. [6–8] (which have been augmented to include the four-loop $\mathcal{O}(\alpha_\mathrm{t}\alpha_\mathrm{s}^3)$ corrections [11] that became available later), the values shown in Fig. 4 are obtained. The dependence of the partial widths on the input parameters m_t, α_s and M_H is relatively mild, leading to variations at the per-mille level within the phenomenologically relevant ranges $165 \ldots 190$ GeV, $0.113 \ldots 0.123$ and $100 \ldots 600$ GeV, respectively.

To illustrate the impact of the newly calculated fermionic two-loop corrections, Tab. 3 shows a comparison to the previously known approximation of the EW two-loop corrections for large values of m_t [15, 16]†. The new results lead to a relative modifications of a few $\times$ 10^{-4}, with the exact value varying depending on the final state. For the total width, the shift is smaller, but comparable to the current experimental measurement, $\Gamma_\mathrm{Z} = (2.4952 \pm 0.0023)$ GeV [1], which has a relative uncertainty of about 10^{-3}.

4.2 Ratios

Instead of directly determining the partial widths for the different final states, the experiments at LEP and SLC obtained values for various branching ratios, since this permits a better control of systematic uncertainties. The most relevant ratios are

$$R_\ell = \Gamma_\mathrm{had}/\Gamma_\ell, \qquad R_c = \Gamma_c/\Gamma_\mathrm{had}, \qquad R_b = \Gamma_b/\Gamma_\mathrm{had}, \tag{27}$$

where $\Gamma_\ell = \frac{1}{3}(\Gamma_e + \Gamma_\mu + \Gamma_\tau)$, and Γ_had is the hadronic partial width, which at parton level is equivalent to $\sum_q \Gamma_q$ ($q = u, d, c, s, b$).

Numerical results for these ratios, with different orders of radiative corrections included, are listed in Tab. 4. Among the three quantities in eq. (27), R_ℓ is shows the most significant effect of the full fermionic EW 2-loop corrections in comparison to the large-m_t approximation, with a relative shift of $\sim 1.4 \times 10^{-4}$. For R_b and R_c the impact of the new corrections mostly cancels in the ratio. The current experimental values are $R_\ell = 20.767 \pm 0.025$, $R_c = 0.1721 \pm 0.0030$, and $R_b = 0.21629 \pm 0.00066$ [1].

†The author is grateful to S. Mishima for supplying these numbers based on the work in Ref. [3].

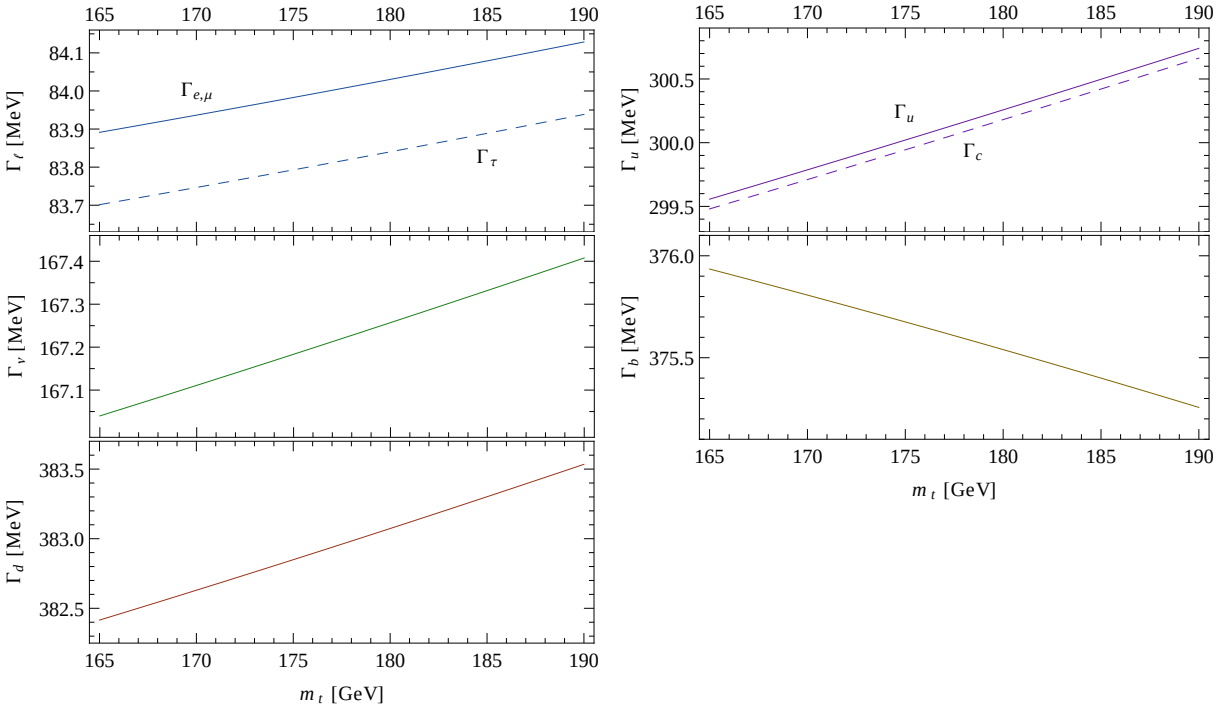

Figure 4: *Results for the Z partial widths Γ_i, with M_{W} calculated from G_μ, using all perturbative corrections discussed in the text and including the full radiator functions $\mathcal{R}_{\mathrm{V,A}}$. The dependence on m_{t} is shown explicitly, while the other input parameters are fixed to the values in Tab. 1.*

Γ_i [GeV]	this work	Large-m_{t} exp. for EW 2-loop
$\Gamma_{e,\mu}$	0.08397	0.08399
Γ_τ	0.08378	0.08380
Γ_ν	0.16716	0.16722
Γ_u	0.29995	0.29996
Γ_c	0.29987	0.29988
$\Gamma_{d,s}$	0.38278	0.38290
Γ_b	0.37573	0.37577
Γ_{Z}	2.49430	2.49485

Table 3: *Comparison between the result based on the full fermionic two-loop EW corrections and the large-m_{t} approximation [3, 15, 16], with M_{W} calculated from G_μ at the same level of precision in each column. In both cases, the complete radiator functions $\mathcal{R}_{\mathrm{V,A}}$ are included. For consistency of the comparison, the relatively small $\mathcal{O}(\alpha_{\mathrm{t}}\alpha_{\mathrm{s}}^3)$ contribution has been removed in the second column, since this part is also missing in the last column.*

	R_ℓ	R_c	R_b
Born $+\,\mathcal{O}(\alpha)$	20.8031	0.17230	0.21558
$+\mathcal{O}(\alpha\alpha_\mathrm{s})$	20.7963	0.17222	0.21593
$+\mathcal{O}(\alpha_\mathrm{t}\alpha_\mathrm{s}^2,\, \alpha_\mathrm{t}\alpha_\mathrm{s}^3,\, \alpha_\mathrm{t}^2\alpha_\mathrm{s},\, \alpha_\mathrm{t}^3)$	20.7943	0.17222	0.21593
$+\mathcal{O}(N_f^2\alpha^2, N_f\alpha^2)$	20.7509	0.17223	0.21580
$-\mathcal{O}(\alpha_\mathrm{t}\alpha_\mathrm{s}^3)$	20.7512	0.17223	0.21580
Large-m_t exp. for EW 2-loop	20.7484	0.17220	0.21579

Table 4: *Results for the ratios R_ℓ, R_c and R_b, with M_W calculated from G_μ to the same order as indicated in each line. In all cases, the complete radiator functions $\mathcal{R}_{\mathrm{V,A}}$ are included. The last two lines compare the new result with the previous calculation using a large-m_t approximation [3,15,16]. For consistency of the comparison, the $\mathcal{O}(\alpha_\mathrm{t}\alpha_\mathrm{s}^3)$ contribution is not included in either of these last two lines.*

Note that the numbers for R_b given here differ somewhat from Ref. [17], which is due to two factors: Firstly, the non-factorizable $\mathcal{O}(\alpha\alpha_\mathrm{s})$ contributions [23,24], as well as higher-order corrections from Ref. [10,11] and $\mathcal{O}(\alpha_\mathrm{s}^4)$ final-state corrections [21] were not included in Ref. [17]. Together, these account for a shift of 2–3 $\times\, 10^{-4}$, depending on the input parameters. Secondly, while in Ref. [17] the perturbative expansion was applied directly to the ratio R_b, the values in Tab. 4 have been obtained using perturbative results for Γ_b and Γ_had, as explained in the previous subsection, and dividing them numerically. The two treatments differ by higher-order terms, and thus this part of the discrepancy should be attributed to the theoretical uncertainty (see section 5).

It is recommended to use the parametrization formula for R_b given in this paper, rather than the one in Ref. [17], since additional higher-order contributions are included here.

4.3 Parametrization formulae

For practical purposes, the complete results for the partial widths, branching ratios, and the peak cross-sections, including all higher-order corrections listed at the beginning of section 4 and M_W calculated from G_μ to the same precision, are most easily represented by a simple parametrization formula. Within currently allowed experimental ranges for the input parameters, the following form provides a very good description:

$$
\begin{aligned}
&X = X_0 + c_1 L_\mathrm{H} + c_2\Delta_\mathrm{t} + c_3\Delta_{\alpha_\mathrm{s}} + c_4\Delta_{\alpha_\mathrm{s}}^2 + c_5\Delta_{\alpha_\mathrm{s}}\Delta_\mathrm{t} + c_6\Delta_\alpha + c_7\Delta_\mathrm{Z}, \qquad (28)\\
&L_\mathrm{H} = \log\frac{M_\mathrm{H}}{125.7\ \mathrm{GeV}}, \quad \Delta_\mathrm{t} = \left(\frac{m_\mathrm{t}}{173.2\ \mathrm{GeV}}\right)^2 - 1, \quad \Delta_{\alpha_\mathrm{s}} = \frac{\alpha_\mathrm{s}(M_\mathrm{Z})}{0.1184} - 1,\\
&\Delta_\alpha = \frac{\Delta\alpha}{0.059} - 1, \quad \Delta_\mathrm{Z} = \frac{M_\mathrm{Z}}{91.1876\ \mathrm{GeV}} - 1.
\end{aligned}
$$

As before, M_H, M_Z, m_t and $\Delta\alpha$ are defined in the on-shell scheme, using the running-width scheme for M_Z (to be consistent with the published experimental values), while α_s is defined in the $\overline{\mathrm{MS}}$ scheme.

Observable	X_0	c_1	c_2	c_3	c_4	c_5	c_6	c_7	max. dev.
$\Gamma_{e,\mu}$ [MeV]	83.966	−0.047	0.807	−0.095	−0.01	0.25	−1.1	285	< 0.001
Γ_τ [MeV]	83.776	−0.047	0.806	−0.095	−0.01	0.25	−1.1	285	< 0.001
Γ_ν [MeV]	167.157	−0.055	1.26	−0.19	−0.02	0.36	−0.1	503	< 0.001
Γ_u [MeV]	299.936	−0.34	4.07	14.27	1.6	1.8	−11.1	1253	< 0.001
Γ_c [MeV]	299.860	−0.34	4.07	14.27	1.6	1.8	−11.1	1253	< 0.001
$\Gamma_{d,s}$ [MeV]	382.770	−0.34	3.83	10.20	−2.4	0.67	−10.1	1469	< 0.001
Γ_b [MeV]	375.724	−0.30	−2.28	10.53	−2.4	1.2	−10.0	1458	< 0.001
$\Gamma_{\rm Z}$ [MeV]	2494.24	−2.0	19.7	58.60	−4.0	8.0	−55.9	9267	< 0.01
R_ℓ $[10^{-3}]$	20750.9	−8.1	−39	732.1	−44	5.5	−358	11702	< 0.1
R_c $[10^{-3}]$	172.23	−0.029	1.0	2.3	1.3	0.38	−1.2	37	< 0.01
R_b $[10^{-3}]$	215.80	0.031	−2.98	−1.32	−0.84	0.035	0.73	−18	< 0.01
$\sigma^0_{\rm had}$ [pb]	41488.4	3.0	60.9	−579.4	38	7.3	85	−86027	< 0.1

Table 5: *Coefficients for the parametrization formula* (28) *for various observables* (X). *Within the ranges* $M_{\rm H} = 125.7 \pm 2.5$ GeV, $m_{\rm t} = 173.2 \pm 2.0$ GeV, $\alpha_{\rm s} = 0.1184 \pm 0.0050$, $\Delta\alpha = 0.0590 \pm 0.0005$ *and* $M_{\rm Z} = 91.1876 \pm 0.0042$ GeV, *the formula approximates the full result with maximal deviations given in the last column.*

The coefficients for the different observables discussed in the previous subsections are given in Tab. 5. With these parameters, the formula provides a very good approximation to the full result within the ranges $M_{\rm H} = 125.7 \pm 2.5$ GeV, $m_{\rm t} = 173.2 \pm 2.0$ GeV, $\alpha_{\rm s} = 0.1184 \pm 0.0050$, $\Delta\alpha = 0.0590 \pm 0.0005$ and $M_{\rm Z} = 91.1876 \pm 0.0042$ GeV, with maximal deviations as quoted in the last column of Tab. 5.

Extended fit formulae, which cover a larger parameter region (in particular larger ranges for $M_{\rm H}$ and $m_{\rm t}$), are given in appendix B.

5 Error estimate

The results presented in this paper have an intrinsic theoretical uncertainty from currently unknown higher-order contributions. The most important missing pieces are the bosonic EW $\mathcal{O}(\alpha^2_{\rm bos})$ corrections (stemming from two-loop diagrams without closed fermion loops), and $\mathcal{O}(\alpha^3)$, $\mathcal{O}(\alpha^2\alpha_{\rm s})$, $\mathcal{O}(\alpha\alpha_{\rm s}^2)$ and $\mathcal{O}(\alpha\alpha_{\rm s}^3)$ corrections beyond the leading $m_{\rm t}^n$ terms from Ref. [9–11].

The second category can be estimated by assuming that the perturbation series follows roughly a geometric series. Thus one obtains

$$\mathcal{O}(\alpha^3) - \mathcal{O}(\alpha^3_{\rm t}) \sim \frac{\mathcal{O}(\alpha^2_{\rm ferm}) - \mathcal{O}(\alpha^2_{\rm t})}{\mathcal{O}(\alpha)} \mathcal{O}(\alpha^2_{\rm ferm}), \tag{29}$$

$\Gamma_{e,\mu\,\tau}$	0.012 MeV	$\Gamma_{u,c}$	0.12 MeV	R_ℓ	5×10^{-3}
Γ_ν	0.014 MeV	Γ_b	0.21 MeV	R_c	5×10^{-5}
$\Gamma_{d,s}$	0.09 MeV	$\Gamma_{\rm Z}$	0.5 MeV	R_b	1.5×10^{-4}

Table 6: *Remaining theory uncertainty for the partial and total Z widths and branching ratios, using the estimation procedure described in the text.*

$$\mathcal{O}(\alpha^2\alpha_{\rm s}) - \mathcal{O}(\alpha_{\rm t}^2\alpha_{\rm s}) \sim \frac{\mathcal{O}(\alpha_{\rm ferm}^2) - \mathcal{O}(\alpha_{\rm t}^2)}{\mathcal{O}(\alpha)}\mathcal{O}(\alpha\alpha_{\rm s}), \tag{30}$$

$$\mathcal{O}(\alpha\alpha_{\rm s}^2) - \mathcal{O}(\alpha_{\rm t}\alpha_{\rm s}^2) \sim \frac{\mathcal{O}(\alpha\alpha_{\rm s}) - \mathcal{O}(\alpha_{\rm t}\alpha_{\rm s})}{\mathcal{O}(\alpha)}\mathcal{O}(\alpha\alpha_{\rm s}), \tag{31}$$

$$\mathcal{O}(\alpha\alpha_{\rm s}^3) - \mathcal{O}(\alpha_{\rm t}\alpha_{\rm s}^3) \sim \frac{\mathcal{O}(\alpha\alpha_{\rm s}) - \mathcal{O}(\alpha_{\rm t}\alpha_{\rm s})}{\mathcal{O}(\alpha)}\mathcal{O}(\alpha\alpha_{\rm s}^2), \tag{32}$$

where the known leading large-$m_{\rm t}$ approximations have been subtracted in the numerators, and $\alpha_{\rm ferm}^2$ indicates the fermionic EW two-loop contribution discussed in this paper, which is currently the only known $\mathcal{O}(\alpha^2)$ piece. Using these expressions, one finds for the total Z width

$$\begin{aligned} \Gamma_{\rm Z}: \qquad & \mathcal{O}(\alpha^3) - \mathcal{O}(\alpha_{\rm t}^3) \sim 0.26 \text{ MeV}, \qquad \mathcal{O}(\alpha^2\alpha_{\rm s}) - \mathcal{O}(\alpha_{\rm t}^2\alpha_{\rm s}) \sim 0.30 \text{ MeV}, \\ & \mathcal{O}(\alpha\alpha_{\rm s}^2) - \mathcal{O}(\alpha_{\rm t}\alpha_{\rm s}^2) \sim 0.23 \text{ MeV}, \qquad \mathcal{O}(\alpha\alpha_{\rm s}^3) - \mathcal{O}(\alpha_{\rm t}\alpha_{\rm s}^3) \sim 0.035 \text{ MeV}. \end{aligned} \tag{33}$$

The error from the missing bosonic $\mathcal{O}(\alpha_{\rm bos}^2)$ contributions can be evaluated by taking the square of the bosonic one-loop corrections. For $\Gamma_{\rm Z}$ this leads to the estimate $\mathcal{O}(\alpha_{\rm bos}^2) \sim 0.1$ MeV.

Besides the EW and mixed EW/QCD vertex corrections, one also has to consider the impact of the unknown $\mathcal{O}(\alpha_{\rm s}^5)$ final-state QCD contribution. Using again the assumption that the perturbative series approximately follows a geometric series, one obtains for the total width

$$\Gamma_{\rm Z}: \quad \mathcal{O}(\alpha_{\rm s}^5) \sim \frac{\mathcal{O}(\alpha_{\rm s}^4)}{\mathcal{O}(\alpha_{\rm s}^3)}\mathcal{O}(\alpha_{\rm s}^4) \approx 0.04 \text{ MeV}. \tag{34}$$

Other higher-order final-state QED and QCD effects, *e. g.* of order $\mathcal{O}(\alpha\alpha_{\rm s}^2)$ or $\mathcal{O}(\alpha^2\alpha_{\rm s})$ are expected to be even smaller by the same assessment method.

Combining eqs. (33) and (34) and the $\mathcal{O}(\alpha_{\rm bos}^2)$ estimate in quadrature, the total theory error adds up to $\delta\Gamma_{\rm Z} \approx 0.5$ MeV.

Applying the same procedure to the partial widths, one obtains the theory errors listed in Table 6. For the ratios (R_ℓ, R_c and R_b), the theory uncertainty has been simply estimated from the partial widths using Gaussian error propagation.

For the hadronic peak cross-section, the theory error can be evaluated from $\sigma_{\rm had}^0 \propto (\Gamma_e\Gamma_{\rm had}/\Gamma_{\rm Z}^2)\,(1 + \delta X)$. In the first term, the impact of perturbative higher-order corrections

partially cancels in the ratio. As a result, the dominant uncertainty stems from the δX term, leading to the estimates

$$\begin{aligned} \sigma^0_{\text{had}}: \qquad \mathcal{O}(\alpha^3) &\sim \sigma^0_{\text{had,Born}} \delta X \frac{\Gamma_{\text{Z}}^{(\alpha^2)}}{\Gamma_{\text{Z}}^{(\alpha)}} \sim 3.7 \text{ pb}, \\ \mathcal{O}(\alpha^2\alpha_{\text{s}}) &\sim \sigma^0_{\text{had,Born}} \delta X \frac{\Gamma_{\text{Z}}^{(\alpha\alpha_{\text{s}})}}{\Gamma_{\text{Z}}^{(\alpha)}} \sim 4.2 \text{ pb}, \end{aligned} \tag{35}$$

where the total width, Γ_{Z}, has been used for the scaling on perturbative orders, since both δX and Γ_{Z} are related to the imaginary part of the Z self-energy. The $\mathcal{O}(\alpha^2_{\text{bos}})$ contribution for σ^0_{had} is estimated by squaring the bosonic one-loop corrections to the partials widths, as above, and using Gaussian error propagation, resulting in an error contribution of about 2 pb. The total theory error follows from combining this with (35) in quadrature, yielding $\delta\sigma^0_{\text{had}} \approx 6$ pb.

6 Summary

In this article, the full electroweak two-loop corrections from diagrams with closed fermion loops to all partial widths of the Z-boson within the Standard Model has been presented. Together with previous results for the effective weak mixing angle [12–14] and the hadronic Z-peak cross-section [18], this provides a complete description of fermionic two-loop corrections to resonant Z-boson production and decay at e^+e^- colliders. Precise predictions are given for the commonly used experimental observables: the total width Γ_{Z}, the branching ratios R_ℓ, R_c and R_b, and the hadronic peak cross-section σ^0_{had}. For convenient use by other researchers, simple parametrization formulas are provided, which accurately reproduce the full result over large ranges of the input parameters.

Electroweak two-loop corrections to the total width, partial widths, branching ratios, and peak cross-sections are sizeable and must be included in phenomenological analyses of LEP1 and SLC data. Compared to previous calculations, which use an expansion for large values of the top-quark mass, the new results lead to moderately small shifts of a few$\times 10^{-4}$ for these observables, thus giving confidence in the robustness of the perturbative expansion.

The added information from the full electroweak two-loop corrections helps to estimate the intrinsic uncertainty from unknown higher-order corrections. The theory error is found to be safely below the current experimental errors for all Z-pole observables. However, additional work will be necessary to match the precision of a future linear e^+e^- collider [37].

As a by-product, an updated result for the branching R_b has been presented, which improves on Ref. [17] by including additional higher-order terms.

Acknowledgments

The author gratefully acknowledges many discussions and detailed numerical comparisons with S. Mishima, and feedback on the manuscript from R. Kogler. This work has been supported in part by the National Science Foundation under grant no. PHY-1212635.

A Final-state QED and QCD corrections

The dominant contributions from final-state QED and QCD radiation can be captured through factorizable radiator functions $\mathcal{R}_{\mathrm{V,A}}$ for the vector and axial-vector part, respectively. They are known up to $\mathcal{O}(\alpha_\mathrm{s}^4)$ for massless final-state quarks and $\mathcal{O}(\alpha_\mathrm{s}^3)$ for terms that depend on the masses of the external quarks [20, 21]. Additionally, the $\mathcal{O}(\alpha^2)$ contributions from diagrams with closed fermion loops [22] are also included here.

Up to the precision required for this project, they read

$$\begin{aligned}
\mathcal{R}_V(s) = 1 &+ \frac{3Q_f^2}{4}\frac{\alpha(s)}{\pi} + \frac{\alpha_\mathrm{s}(s)}{\pi} - \frac{Q_f^2}{4}\frac{\alpha(s)}{\pi}\frac{\alpha_\mathrm{s}(s)}{\pi} + Q_f^2\big[C_{\gamma 2} + 2C_2^\mathrm{t}(s/m_\mathrm{t}^2)\big]\Big(\frac{\alpha(s)}{\pi}\Big)^2 \\
&+ \big[C_{02} + C_2^\mathrm{t}(s/m_\mathrm{t}^2)\big]\Big(\frac{\alpha_\mathrm{s}(s)}{\pi}\Big)^2 + C_{03}\Big(\frac{\alpha_\mathrm{s}(s)}{\pi}\Big)^3 + C_{04}\Big(\frac{\alpha_\mathrm{s}(s)}{\pi}\Big)^4 \\
&+ 12\frac{m_f^2}{s}\frac{\alpha_\mathrm{s}(s)}{\pi} - 6\frac{m_f^4}{s^2}\,, \qquad (36)\\
\mathcal{R}_A(s) = 1 &+ \frac{3Q_f^2}{4}\frac{\alpha(s)}{\pi} + \frac{\alpha_\mathrm{s}(s)}{\pi} - \frac{Q_f^2}{4}\frac{\alpha(s)}{\pi}\frac{\alpha_\mathrm{s}(s)}{\pi} + Q_f^2\big[C_{\gamma 2} + 2C_2^\mathrm{t}(s/m_\mathrm{t}^2)\big]\Big(\frac{\alpha(s)}{\pi}\Big)^2 \\
&+ \big[C_{02} + C_2^\mathrm{t}(s/m_\mathrm{t}^2) \pm I_2(s/m_\mathrm{t}^2)\big]\Big(\frac{\alpha_\mathrm{s}(s)}{\pi}\Big)^2 + \big[C_{03} \pm I_3(s/m_\mathrm{t}^2)\big]\Big(\frac{\alpha_\mathrm{s}(s)}{\pi}\Big)^3 \\
&+ \big[C_{04} \pm I_4(s/m_\mathrm{t}^2)\big]\Big(\frac{\alpha_\mathrm{s}(s)}{\pi}\Big)^4 - 6\frac{m_f^2}{s} - 22\frac{m_f^2}{s}\frac{\alpha_\mathrm{s}(s)}{\pi} + 6\frac{m_f^4}{s^2}\,, \qquad (37)
\end{aligned}$$

where contributions of $\mathcal{O}(m_f^6)$, $\mathcal{O}(m_f^4\alpha_\mathrm{s})$, $\mathcal{O}(m_f^2\alpha_\mathrm{s}^2)$, and $\mathcal{O}(m_f^2\alpha)$ have been neglected. For $f = e,\, \mu,\, \tau$ the terms with α_s vanish. In the expressions above, Q_f is the electric charge of the fermion f, the $\pm$ sign applies to down/up-type fermions, and

$$\begin{aligned}
C_{\gamma 2} &= -\frac{55}{6} + \frac{20}{3}\zeta_3, && (38)\\
C_{02} &= \frac{365}{24} - 11\zeta_3 + \Big(-\frac{11}{12} + \frac{2}{3}\zeta_3\Big)n_q, && (39)\\
C_2^\mathrm{t}(x) &= x\Big(\frac{44}{675} - \frac{2}{135}\log x\Big) + \mathcal{O}(x^2), && (40)\\
C_{03} &= -6.63694 - 1.20013 n_q - 0.005178 n_q^2, && (41)\\
C_{04} &= -156.61 + 18.77 n_q - 0.7974 n_q^2 + 0.0215 n_q^3, && (42)\\
I_2(x) &= -\frac{37}{12} + \log x + \frac{7}{81}x + \frac{79}{6000}x^2 + \mathcal{O}(x^3), && (43)\\
I_3(x) &= -15.9877 + \frac{67}{18}\log x + \frac{23}{12}\log^2 x + \mathcal{O}(x), && (44)\\
I_4(x) &= 49.0309 - 17.6637\log x + 14.6597\log^2 x + 3.6736\log^3 x + \mathcal{O}(x), && (45)
\end{aligned}$$

where $n_q = 5$ is the number of light quarks.

In addition, there exists a singlet vector correction, which cannot be assigned to individual partial widths, but only to the total hadronic Z decay [20, 21]. It first enters at $\mathcal{O}(\alpha_\mathrm{s}^3)$ and is numerically very small, so that it can be neglected for the purposes of this analysis.

B Extended parametrization formulae

In section 4.3, the numerical results for the Z-boson partial widths, branching ratio, and peak cross-section were presented in terms of a simple parametrization formula, which provides an accurate description within current allowed ranges for the SM input parameters. However, in global SM fits the results may be needed over a larger range of input parameters. For this purpose the following formula with additional coefficients is introduced:

$$\begin{aligned} X = {} & X_0 + a_1 L_\mathrm{H} + a_2 L_\mathrm{H}^2 + a_3 \Delta_\mathrm{H} + a_4 \Delta_\mathrm{H}^2 + a_5 \Delta_\mathrm{t} + a_6 \Delta_\mathrm{t}^2 + a_7 \Delta_\mathrm{t} L_\mathrm{H} + a_8 \Delta_\mathrm{t} L_\mathrm{H}^2 \\ & + a_9 \Delta_{\alpha_\mathrm{s}} + a_{10} \Delta_{\alpha_\mathrm{s}}^2 + a_{11} \Delta_{\alpha_\mathrm{s}} L_\mathrm{H} + a_{12} \Delta_{\alpha_\mathrm{s}} \Delta_\mathrm{t} + a_{13} \Delta_\alpha + a_{14} \Delta_\alpha L_\mathrm{H} + a_{15} \Delta_\mathrm{Z}, \end{aligned} \tag{46}$$

$$L_\mathrm{H} = \log \frac{M_\mathrm{H}}{125.7\ \mathrm{GeV}}, \quad \Delta_\mathrm{H} = \frac{M_\mathrm{H}}{125.7\ \mathrm{GeV}} - 1, \quad \Delta_\mathrm{t} = \left(\frac{m_\mathrm{t}}{173.2\ \mathrm{GeV}}\right)^2 - 1,$$

$$\Delta_{\alpha_\mathrm{s}} = \frac{\alpha_\mathrm{s}(M_\mathrm{Z})}{0.1184} - 1, \quad \Delta_\alpha = \frac{\Delta\alpha}{0.059} - 1, \quad \Delta_\mathrm{Z} = \frac{M_\mathrm{Z}}{91.1876\ \mathrm{GeV}} - 1.$$

Its range of validity is 70 GeV $< M_\mathrm{H} <$ 1000 GeV, 165 GeV $< m_\mathrm{t} <$ 190 GeV, $\alpha_\mathrm{s} = 0.1184 \pm 0.0050$, $\Delta\alpha = 0.0590 \pm 0.0005$ and $M_\mathrm{Z} = 91.1876 \pm 0.0084$ GeV, with the coefficients and maximal numerical deviations given in Tab. 7.

References

[1] S. Schael *et al.* [ALEPH and DELPHI and L3 and OPAL and SLD and LEP Electroweak Working Group and SLD Electroweak Group and SLD Heavy Flavour Group Collaborations], Phys. Rept. **427**, 257 (2006).

[2] M. Baak *et al.*, Eur. Phys. J. C **72**, 2205 (2012).

[3] M. Ciuchini, E. Franco, S. Mishima and L. Silvestrini, JHEP **1308**, 106 (2013).

[4] J. Beringer *et al.* [Particle Data Group Collaboration], Phys. Rev. D **86**, 010001 (2012).

[5] A. Djouadi and C. Verzegnassi, Phys. Lett. B **195**, 265 (1987); A. Djouadi, Nuovo Cim. A **100**, 357 (1988); B. A. Kniehl, Nucl. Phys. B **347**, 86 (1990); B. A. Kniehl and A. Sirlin, Nucl. Phys. B **371**, 141 (1992); A. Djouadi and P. Gambino, Phys. Rev. D **49**, 3499 (1994) [Erratum-ibid. D **53**, 4111 (1996)].

[6] A. Freitas, W. Hollik, W. Walter and G. Weiglein, Phys. Lett. B **495**, 338 (2000) [Erratum-ibid. B **570**, 260 (2003)]; M. Awramik and M. Czakon, Phys. Rev. Lett. **89**, 241801 (2002), Phys. Lett. B **568**, 48 (2003); A. Onishchenko and O. Veretin, Phys. Lett. B **551**, 111 (2003).

[7] A. Freitas, W. Hollik, W. Walter and G. Weiglein, Nucl. Phys. B **632**,189 (2002) [Erratum-ibid. B **666**, 305 (2003)].

[8] M. Awramik, M. Czakon, A. Freitas and G. Weiglein, Phys. Rev. D **69**, 053006 (2004).

Observable	X_0	a_1	a_2	a_3	a_4	a_5	a_6	a_7
$\Gamma_{e,\mu}$ [MeV]	83.966	−0.1017	−0.06352	0.05500	−0.00145	0.8051	−0.027	−0.017
Γ_τ [MeV]	83.776	−0.1016	−0.06339	0.05488	−0.00145	0.8036	−0.026	−0.017
Γ_ν [MeV]	167.157	−0.1567	−0.1194	0.1031	−0.00269	1.258	−0.13	−0.020
Γ_u [MeV]	299.936	−0.5681	−0.2636	0.2334	−0.00592	4.057	−0.50	−0.058
Γ_c [MeV]	299.859	−0.5680	−0.2635	0.2334	−0.00592	4.056	−0.50	−0.058
$\Gamma_{d,s}$ [MeV]	382.770	−0.6199	−0.3182	0.2800	−0.00711	3.810	−0.25	−0.060
Γ_b [MeV]	375.723	−0.5744	−0.3074	0.2725	−0.00703	−2.292	−0.027	−0.013
$\Gamma_{\rm Z}$ [MeV]	2494.24	−3.725	−2.019	1.773	−0.04554	19.63	−2.0	−0.36
R_ℓ [10^{-3}]	20750.9	−10.00	−1.83	1.878	−0.0343	−38.8	−11	1.2
R_c [10^{-3}]	172.23	−0.034	−0.0058	0.0054	−0.00012	1.00	−0.15	−0.0074
R_b [10^{-3}]	215.80	0.036	0.0057	−0.0044	6.2×10^{-5}	−2.98	0.20	0.020
$\sigma^0_{\rm had}$ [pb]	41488.4	3.88	0.829	−0.911	0.0076	61.10	16	−2.0

Observable	a_8	a_9	a_{10}	a_{11}	a_{12}	a_{13}	a_{14}	a_{15}	max. dev.
$\Gamma_{e,\mu}$ [MeV]	0.0066	−0.095	−0.010	−0.015	0.23	−1.1	0.064	285	< 0.0015
Γ_τ [MeV]	0.0066	−0.095	−0.010	−0.015	0.23	−1.1	0.064	285	< 0.0015
Γ_ν [MeV]	0.0133	−0.19	−0.018	−0.021	0.34	−0.084	0.064	503	< 0.002
Γ_u [MeV]	0.0352	14.26	1.6	−0.081	1.7	−11.1	0.19	1251	< 0.006
Γ_c [MeV]	0.0352	14.26	1.6	−0.081	1.7	−11.1	0.19	1251	< 0.006
$\Gamma_{d,s}$ [MeV]	0.0420	10.20	−2.4	−0.083	0.65	−10.1	0.19	1468	< 0.006
Γ_b [MeV]	0.0428	10.53	−2.4	−0.088	1.2	−10.1	0.19	1456	< 0.006
$\Gamma_{\rm Z}$ [MeV]	0.257	58.60	−4.1	−0.53	7.6	−56.0	1.3	9256	< 0.04
R_ℓ [10^{-3}]	0.72	732.1	−44	−0.64	5.6	−357	−4.7	11771	< 0.15
R_c [10^{-3}]	0.00091	2.3	1.3	−0.0013	0.35	−1.2	0.014	37	< 0.01
R_b [10^{-3}]	−0.00036	−1.3	−0.84	−0.0019	0.054	0.73	−0.011	−18	< 0.01
$\sigma^0_{\rm had}$ [pb]	−0.59	−579.4	38	−0.26	6.5	84	9.5	−86152	< 0.25

Table 7: *Coefficients for the parametrization formula* (46) *for various observables* (X). *Within the ranges* 70 GeV $< M_{\rm H} <$ 1000 GeV, 165 GeV $< m_{\rm t} <$ 190 GeV, $\alpha_{\rm s} = 0.1184 \pm 0.0050$, $\Delta\alpha = 0.0590 \pm 0.0005$ *and* $M_{\rm Z} = 91.1876 \pm 0.0084$ GeV, *the formula approximates the full result with maximal deviations given in the last column.*

[9] L. Avdeev, J. Fleischer, S. Mikhailov and O. Tarasov, Phys. Lett. B **336**, 560 (1994) [Erratum-ibid. B **349**, 597 (1994)]; K. G. Chetyrkin, J. H. Kühn and M. Steinhauser, Phys. Lett. B **351**, 331 (1995); Phys. Rev. Lett. **75**, 3394 (1995).

[10] J. J. van der Bij, K. G. Chetyrkin, M. Faisst, G. Jikia and T. Seidensticker, Phys. Lett. B **498**, 156 (2001); M. Faisst, J. H. Kühn, T. Seidensticker and O. Veretin, Nucl. Phys. B **665**, 649 (2003).

[11] Y. Schröder and M. Steinhauser, Phys. Lett. B **622**, 124 (2005); K. G. Chetyrkin, M. Faisst, J. H. Kühn, P. Maierhoefer and C. Sturm, Phys. Rev. Lett. **97**, 102003 (2006); R. Boughezal and M. Czakon, Nucl. Phys. B **755**, 221 (2006).

[12] M. Awramik, M. Czakon, A. Freitas, G. Weiglein, Phys. Rev. Lett. **93**, 201805 (2004); M. Awramik, M. Czakon and A. Freitas, Phys. Lett. B **642**, 563 (2006); W. Hollik, U. Meier and S. Uccirati, Nucl. Phys. B **731**, 213 (2005); Nucl. Phys. B **765**, 154 (2007).

[13] M. Awramik, M. Czakon and A. Freitas, JHEP **0611**, 048 (2006).

[14] M. Awramik, M. Czakon, A. Freitas and B. A. Kniehl, Nucl. Phys. B **813**, 174 (2009).

[15] G. Degrassi, P. Gambino and A. Vicini, Phys. Lett. B **383**, 219 (1996); G. Degrassi, P. Gambino and A. Sirlin, Phys. Lett. B **394**, 188 (1997); G. Degrassi and P. Gambino, Nucl. Phys. B **567**, 3 (2000).

[16] R. Barbieri, M. Beccaria, P. Ciafaloni, G. Curci and A. Vicere, Phys. Lett. B **288**, 95 (1992) [Erratum-ibid. B **312**, 511 (1993)]; Nucl. Phys. B **409**, 105 (1993); J. Fleischer, O. V. Tarasov and F. Jegerlehner, Phys. Lett. B **319**, 249 (1993); Phys. Rev. D **51**, 3820 (1995).

[17] A. Freitas and Y.-C. Huang, JHEP **1208**, 050 (2012) [Errata ibid. **1305**, 074 (2013), **1310**, 044 (2013)].

[18] A. Freitas, arXiv:1310.2256 [hep-ph].

[19] S. Willenbrock and G. Valencia, Phys. Lett. B **259**, 373 (1991); A. Sirlin, Phys. Rev. Lett. **67**, 2127 (1991); R. G. Stuart, Phys. Lett. B **262**, 113 (1991); P. Gambino and P. A. Grassi, Phys. Rev. D **62**, 076002 (2000).

[20] K. G. Chetyrkin, J. H. Kühn and A. Kwiatkowski, Phys. Rept. **277**, 189 (1996).

[21] P. A. Baikov, K. G. Chetyrkin and J. H. Kühn, Phys. Rev. Lett. **101**, 012002 (2008); P. A. Baikov, K. G. Chetyrkin, J. H. Kühn and J. Rittinger, Phys. Rev. Lett. **108**, 222003 (2012).

[22] A. L. Kataev, Phys. Lett. B **287**, 209 (1992).

[23] A. Czarnecki and J. H. Kühn, Phys. Rev. Lett. **77**, 3955 (1996); R. Harlander, T. Seidensticker and M. Steinhauser, Phys. Lett. B **426**, 125 (1998).

[24] J. Fleischer, O. V. Tarasov, F. Jegerlehner and P. Raczka, Phys. Lett. B **293**, 437 (1992); G. Buchalla and A. J. Buras, Nucl. Phys. B **398**, 285 (1993); G. Degrassi, Nucl. Phys. B **407**, 271 (1993); K. G. Chetyrkin, A. Kwiatkowski and M. Steinhauser, Mod. Phys. Lett. A **8**, 2785 (1993).

[25] D. Bardin *et al.*, in *Reports of the Working Group on Precision Calculations for the Z Resonance*, eds. D. Bardin, W. Hollik and G. Passarino, report CERN 95-03 (1995), pp. 7–162.

[26] P. A. Grassi, B. A. Kniehl and A. Sirlin, Phys. Rev. Lett. **86**, 389 (2001).

[27] T. Hahn, Comput. Phys. Commun. **140**, 418 (2001).

[28] M. L. Nekrasov, Phys. Lett. B **531**, 225 (2002).

[29] G. Weiglein, R. Scharf and M. Bohm, Nucl. Phys. B **416**, 606 (1994).

[30] K. G. Chetyrkin and F. V. Tkachov, Nucl. Phys. B **192**, 159 (1981); S. Laporta, Int. J. Mod. Phys. A **15**, 5087 (2000).

[31] T. Gehrmann and E. Remiddi, Nucl. Phys. B **580**, 485 (2000).

[32] S. Bauberger, F. A. Berends, M. Böhm and M. Buza, Nucl. Phys. B **434**, 383 (1995); S. Bauberger and M. Böhm, Nucl. Phys. B **445**, 25 (1995).

[33] A. Freitas, JHEP **1207**, 132 (2012) [Erratum-ibid. **1209**, 129 (2012)].

[34] F. Jegerlehner, Eur. Phys. J. C **18**, 673 (2001).

[35] M. Steinhauser, Phys. Lett. B **429**, 158 (1998).

[36] M. Davier, A. Hoecker, B. Malaescu and Z. Zhang, Eur. Phys. J. C **71**, 1515 (2011) [Erratum-ibid. C **72**, 1874 (2012)]; K. Hagiwara, R. Liao, A. D. Martin, D. Nomura and T. Teubner, J. Phys. G **38**, 085003 (2011); H. Burkhardt and B. Pietrzyk, Phys. Rev. D **84**, 037502 (2011).

[37] A. Freitas, K. Hagiwara, S. Heinemeyer, P. Langacker, K. Moenig, M. Tanabashi and G. W. Wilson, arXiv:1307.3962.